Effect of secondary electrons on the patch formation in insulating capillaries by ion beams

E. Giglio ●* and T. Le Cornu

Centre de Recherche sur les Ions, les Matériaux et la Photonique (CIMAP), Normandie Université, ENSICAEN, UNICAEN, CEA, CNRS,
F-14000 Caen, France

The transmission rate of a low-energy Ar^{q+} ion beam through a macroscopic glass tube of large aspect ratio is simulated. Secondary electron (SE) emission, induced by ion impacts with the inner surface of the capillary, are taken explicitly into account by adding a SE source term to the charge dynamics equation. We find that the additional SE channel significantly alters the distribution of the deposited charge in the capillary wall. Compared to the case without the SE channel, the electric field generated by the self-organized charge patches is generally weaker, yielding drastically different transmission rates, especially for higher beam intensities. The effect of SEs on the patch formation and resulting transmission rate is found to be significant for SE yields as low as 1 SE per ion impact, in the case of Ar^+ ions. We propose a numerical experiment that can be tested experimentally, potentially allowing us to conclude if the SE channel is indeed crucial for accurately simulating the guiding of an ion beam through insulating capillaries. In the long run, our simulations may provide theoretical support for measuring the SE yield of low-energy ions impacting insulating surfaces at grazing angles.

I. INTRODUCTION

Guiding of low-energy ions by insulating capillaries was first reported by Stolterfoht *et al.* in 2002 for microcapillaries [1] and later by Ikeda *et al.* [2] for macroscopic glass capillaries. They found that even though the capillaries were tilted with respect to the beam axis such as no geometrical transmission was allowed, the beam was steered after an initial charge-up phase through the insulating capillary by self-organized charge patches. As a result, a part of the beam could be transmitted, with the ions keeping their initial charge state, indicating that the ions never touched the inner wall.

In the past, several authors modeled and simulated the guiding of the injected beam through insulating capillaries. In pioneering simulations, Schiessl *et al.* allowed the deposited charges to diffuse along the inner surface of the nanocapillary and through the bulk. Assuming an exponential decay of the deposited charges with a rate proportional to the bulk conductivity, they succeeded in qualitatively reproducing the observed trends in polyethylene terephthalate (PET) nanocapillaries [3]. As diffusion currents are rapidly dominated by drift currents in the presence of electric fields, a different approach was adopted in [4–6]. In the latter, surface currents were described involving a nonlinear charge drift model, where the accumulated charge carriers were field driven along the surface, with a velocity proportional to their surface mobility. For macroscopic glass capillaries, surface currents were assumed to have no dominant contribution in the charge dynamics and observed trends in macroscopic glass capillaries were qualitatively reproduce by simply adjusting the rate of the exponential charge decay [7,8].

Recently, we presented a model accounting for the dynamics of the deposited charges by means of solving the continuity equations for surface charges at the capillary interfaces. The model, labeled INCA4D, depends explicitly on the bulk and surface conductivity of the capillary, which must be provided. The model was successfully used to simulate the radial focusing in tapered capillaries [9,10]. The simulated and experimental results given in [9] agreed convincingly well, giving confidence that the model reliably describes the charge dynamics in insulating glass capillaries.

The same numerical code was then used to theoretically support the observed decay rates of charge patches in tilted glass tubes [11]. While for injected beam intensities below 4 pA the code qualitatively reproduced the observed time evolution of the transmitted fraction, the model predicted a blocking of the transmission for injected intensities above 8 pA. But that result was in disagreement with the observed data. Experimentally, the transmitted beam did not experience any blocking for injected intensities as high as 35 pA.

Initially, we thought that the culprit for the discrepancy was the value of the surface conductivity used in the model. Indeed, the surface conductivity in glass capillaries is usually not a well-known quantity, as it strongly depends on the surface contamination. We thus varied the surface conductivity in our simulations over three orders of magnitude. But even then, we could not find a single value for the surface conductivity that was able to reproduce, even quantitatively, the observed transmission rates presented in [11], namely, for intensities as low as 0.3 pA and as high as 35 pA. For completeness, we even varied the bulk conductivity in the simulations, which was also unsuccessful. We concluded then that a channel must be missing in the charge dynamics, which seems to be important especially at high beam intensities.

A source term that we neglected up to now in the charge dynamics is one that accounts for secondary electrons (SEs).

---

*Corresponding author: giglio@ganil.fr

When beam ions hit the inner insulating surface of the capillary, SEs are possibly emitted from the impact point with a given initial velocity, guided by the electric field and eventually absorbed by the surface at different locations. Schliessl *et al.* already included a SE source term in their model to simulate the electron transmission through insulating Mylar capillaries [12]. Also, preliminary calculations including a SE source were presented in [11], where the added SE source term was shown to have a non-negligible effect on the transmission rate.

In the present work, we investigate the influence of the SE channel on the charge patch formation by monitoring the transmitted beam current through a straight glass capillary, tilted with respect to the beam axis. We want to identify experimental conditions for which the transmission rate is sensitive to SE yields. The aim is to make a numerical prediction with our code that could be verified (or falsified) experimentally. It will hopefully allow us to conclude if adding a SE channel to the charge dynamics is mandatory. If experimental results were to confirm the numerical predictions, it would mean a new milestone in the modeling of the self-organized guiding of ion beams by insulating capillaries. Last, but not least, the presented numerical results could help deduce the SE yield by low-energy ions impacting insulating surfaces at grazing angles, simply by recording in time the transmitted beam fraction.

II. MODELING

A. Surface charge dynamics

We propose to simulate the transmission of a low-energy Ar^{q+} ion beam through a macroscopic borosilicate glass tube of dielectric constant $\varepsilon_r = 4.8$. For the present work, we consider a capillary tube of length $H = 60$ mm, inner radius of $R_1 = 0.43$ mm, and an outer radius of $R_2 = 0.75$ mm, matching the dimensions of the glass tubes sold by Warner Instruments [13]. The outer surface, including the entrance and outlet, is metallized and electrically grounded. The surface charge dynamics, on which the simulations are based, was already discussed in [14,15]. Here we merely give a brief summary. Cylindrical coordinates (r, θ, z) are used throughout the paper. The injected charges are assumed to accumulate only at the inner interface, so that the electric field in the bulk (E_r, E_θ, E_z) is divergence free. The dynamics of the surface charge density σ at the inner surface $(r = R_1)$ of the capillary tube is given by the charge conservation equation,

$$\frac{\partial \sigma}{\partial t} + \kappa_s \left(\frac{1}{R_1} \frac{\partial E_\theta}{\partial \theta} + \frac{\partial E_z}{\partial z} \right) = -\kappa_b E_r + \gamma. \quad (1)$$

The first right-hand term stands for the charges that are field driven from the inner to the outer grounded surface. The current density through the bulk is proportional to the bulk conductivity κ_b, which is considered constant. The second left-hand term describes the charge migration along the inner surface, in the angular and axial direction, and is proportional to the surface conductivity κ_s. In agreement with the measurement done by Gruber *et al.* [16], we take, for borosilicate glass, the common values of $\kappa_b = 10^{-13}$ S/m and $\kappa_s = 10^{-16}$ S. The source term γ accounts for the current density of injected holes and electrons at the interface.

TABLE I. Relaxation rates τ_{mn}^{-1} (in mHz) for angular indexes $0 \leqslant m \leqslant M = 6$, as well as for three different axial indexes, $n = 1, 2, 10$.

n	τ_{0n}^{-1}	τ_{1n}^{-1}	τ_{2n}^{-1}	τ_{3n}^{-1}	τ_{4n}^{-1}	τ_{5n}^{-1}	τ_{6n}^{-1}
1	2.5	4.9	10	15.4	20.5	25.5	30.3
2	2.5	4.9	10	15.4	20.5	25.5	30.3
10	2.6	5	10	15.4	20.5	25.5	30.3

Using a two-dimensional (2D) Fourier transform, Eq. (1) may be conveniently solved in terms of moments of the charge distribution. Here we merely give the starting point and the main result; a detailed discussion can be found in [14,15]. The surface charge density σ and the source term γ may be decomposed on moments with angular and axial indexes m and n,

$$\begin{bmatrix} \sigma(\theta, z, t) \\ \gamma(\theta, z, t) \end{bmatrix} = \sum_{m=0}^{M} \sum_{n=1}^{N} \begin{bmatrix} \sigma_{mn}(t) \\ \gamma_{mn}(t) \end{bmatrix} \cos(m\theta) \sin(k_n z), \quad (2)$$

with $k_n = n\pi/H$. The chosen basis assumes xOz plane symmetry and zero deposited charges at the grounded entrance $(z = 0)$ and outlet $(z = H)$. The simulated results presented in Sec. III used $M = 6$ and $N = 400$, corresponding to a spatial resolution of less than 200 μm in both directions. By following the steps outlined in [14,15], one obtains the dynamics of each moment σ_{mn},

$$\frac{\partial \sigma_{mn}(t)}{\partial t} = \frac{-\sigma_{mn}(t)}{\tau_{mn}} + \gamma_{mn}(t). \quad (3)$$

Remarkably, each moment σ_{mn} is independent from the others and is characterized by its proper relaxation time τ_{mn}. The latter merely depends on the electric properties $(\kappa_b, \kappa_s, \varepsilon_r)$ and geometric dimensions (R_1, R_2, H) of the capillary and all can be calculated once for each of the indexes (m, n). Table I gives some relevant relaxation rates that characterize the present capillary. Eventually, Eq. (3) can be solved numerically using a first-order exponential integrator method,

$$\sigma_{mn}(t + \Delta t) = \sigma_{mn}(t)e^{-\frac{\Delta t}{\tau_{mn}}} + \tau_{mn}\left(1 - e^{-\frac{\Delta t}{\tau_{mn}}}\right)\gamma_{mn}(t), \quad (4)$$

where $\gamma_{mn}(t)$ is supposedly constant during the time step Δt.

The analysis of the charge dynamics in terms of moments is extremely powerful, but would go beyond the scope of this paper. Here we highlight only two properties: the total charge of a patch in the capillary is given by the monopole moments $(m = 0)$, which decay with a rate of about 2.5 mHz or, equivalently, with a relaxation time of 400 s. The electric field responsible for the beam deflection is generated by charge moments with higher angular indexes $(m \geqslant 1)$. Their rates increase only slightly with the axial index n, but increase grossly linearly with the angular index $m \geqslant 1$. This indicates that the moments σ_{mn} with $m \geqslant 1$ decay predominantly due to charge migration along the inner surface in the angular direction. The latter is controlled by the surface conductivity κ_s.

B. Ion trajectories

The beam ions are propagated classically using the Hamiltonian equation of motion (EOM). Inside the capillary, the ions feel only the electric field generated by the charge accumulated in the capillary wall. The trajectories do not depend on the charge over mass ratio of the ion, as can be easily seen by putting the EOM into a dimensionless form; see Appendix 1. The initial positions and velocities are sampled as follows: the ions are emitted from a source located 50 cm upstream from the capillary entrance. The source is represented by a disk having a diameter of 2 mm, on which the ions are uniformly sampled. The angle between the initial velocity vector and the beam axis is sampled according to a normal distribution having a FWHM of $0.3°$. The projectiles that, after traveling through the 50 cm field-free region, miss the entrance of the capillary are discarded. Only the trajectories that pass the 0.8 mm $\varnothing$ collimator hole in front of the capillary are retained in the calculation. With this method, the injected beam is characterized by divergence with a half-opening angle of $0.36°$ and a rms emittance [17] of 0.5 mm mrad. For more details, see [10].

C. Secondary electrons

We assume that each Ar^{q+} ion that is not transmitted, but hits the inner capillary surface, injects $q + N_{SE}$ holes at the impact point, which are immediately trapped by hole centers of the insulator. [Factually, in order to speed up the simulations, each ion injects $q_r(q + N_{SE})$ holes at the impact point, where $q_r = 2000$ is the speed-up factor. This amounts to saying that each simulated trajectory stands for 2000 ion trajectories.] Among the $q + N_{SE}$ electrons that are ejected from the impact point, q are picked up by the impacting Ar^{q+} projectile, which becomes neutralized and will no longer be considered. The remaining N_{SE} electrons are field driven through the capillary until they hit the inner surface and are reabsorbed at a new location or escape the capillary. The number of ions per unit time that enter the capillary is $I_{in}/(qe)$, where e is the elementary charge and I_{in} is the injected intensity. The source term thus becomes

$$\gamma_{mn}(t) = \frac{I_{in}}{qe}\left[e(q + N_{SE})\gamma_{mn}^h(t) - eN_{SE}\gamma_{mn}^e(t)\right]$$
$$= I_{in}\left\{\gamma_{mn}^h(t) + \frac{N_{SE}}{q}\left[\gamma_{mn}^h(t) - \gamma_{mn}^e(t)\right]\right\}, \quad (5)$$

where $\gamma_{mn}^h(t)$ and $\gamma_{mn}^e(t)$ are the moments of the probability distribution per unit surface for the injection of holes and electrons at time t, respectively. From Eq. (5), we note that the SE channel is only active if the difference $\gamma_{mn}^h - \gamma_{mn}^e$ is nonzero or, alternatively, if the electrons are injected at sufficiently different locations than the holes. We also note that the SE channel is controlled by the ratio N_{SE}/q. This has an interesting consequence: the source term for (i) Ar^+ ions that emit, on average, 1 SE per impact and (ii) Ar^{3+} ions that emit, on average, 3 SEs per impact is eventually the same. Further, highly charged ions, which are expected to generate a number of SEs, N_{SE}, roughly proportional to the ion charge q for a given impact velocity (see Fig. 3 in [18]), may finally have a ratio N_{SE}/q similar to that of singly charged ions.

The authors are not aware of published angular and energy distributions of SE emission from borosilicate glass induced by Ar^{q+} projectiles in the keV range and at grazing angles. The initial conditions of the SEs are thus chosen using commonly observed distributions: the fraction of electrons, leaving a surface element within a narrow angle $d\phi$ in a direction making an angle ϕ to the surface normal, follows a Knudsen cosine law [19], where $\sin(2\phi)d\phi$ gives the fraction of electrons that have velocity vectors between $\phi + d\phi$ [20]. The initial energy ξ of the SEs is chosen randomly according to the probability law [21],

$$P(\xi + d\xi) = \frac{\xi}{\xi_0^2}\exp\left(-\frac{\xi}{\xi_0}\right)d\xi, \quad \xi_0 = 2 \text{ eV}, \quad (6)$$

which fits reasonably well with the energy spectrum of electrons emitted from an Al-Mg (15%) alloy bombarded by 50 keV Ar^+ ions [22], as well as the calculated energy distribution of SE emission from amorphous SiO_2 [23]. It should be mentioned that the distributions for the initial conditions for SEs are just estimates, but could be improved in the future.

III. SIMULATED RESULTS

In this study, we want to provide simulated results that are sensitive to the absence or presence of the SE channel, so that experimental measurements are able to discriminate between both approaches. Actually, transmitted beam intensities I_{out} can be measured rather precisely. We thus propose to check how far SEs influence the transmission rates. To that end, we propose to simulate the transmission of a 2.5 keV Ar^+ beam through the borosilicate glass tube, thus setting $q = 1$ and $N_{SE}/q = N_{SE}$. The choice of singly charged Ar^+ projectiles is motivated by our existing experimental setup in CIMAP. Nevertheless, we want to emphasize that the following simulated results are also valid for multiply charged Ar^{q+} ions, as long as the extraction potential of the ion source is kept to $U_s = 2500$ V; see the dimensionless charge dynamics in Appendix 2. Just keep in mind that in the following figures and discussions, N_{SE} is to be understood as the number of SEs emitted per impact and per charge state q. For example, simulations with Ar^+ emitting $N_{SE} = 1$ are also valid for Ar^{3+} emitting three SEs per impact, while simulations with Ar^+ emitting, on average, 1/2 SE are also valid for Ar^{6+} emitting three SEs per impact.

The capillary has an aspect ratio of 70 and is characterized by a geometrical transmission angle of $0.8°$. The capillary is tilted by $4°$ with respect to the beam axis, so that no geometrical transmission is possible. The injected beam is collimated to a diameter of 0.8 mm. The average number N_{SE} of emitted SEs per impact depends on the charge state and kinetic energy of the projectile, its incidence angle with the surface, as well as the nature of the insulator. As we did not find measurements of the SE yield for keV Ar^{q+} ions hitting a glass surface at grazing angles, we investigate the transmission rate for different values of N_{SE}/q, namely, 1/2, 1, 2, 3, and 4. This should allow us to cover the expected range of SE per impact and give possible trends. Our numerical code INCA4D is rather CPU efficient, 6×10^6 trajectories per 24 h, allowing us to explore times T more than twice the longest charge relaxation
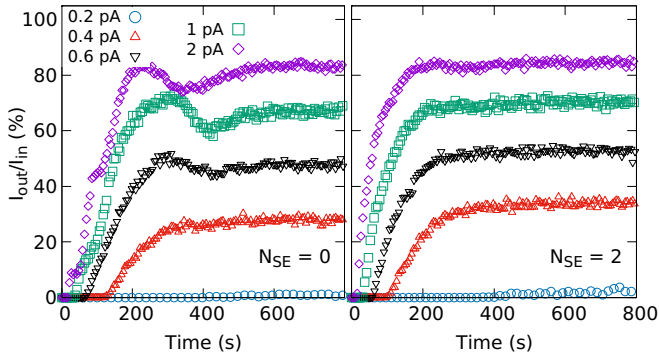
FIG. 1. Simulated transmitted fraction of a 2.5 keV Ar$^+$ ion beam through the 4° tilted capillary as a function of the time for different current intensities I_{in} ranging from 0.2 to 2 pA. Left panel: $N_{SE} = 0$; right panel: $N_{SE} = 2$.

time of the system, $T \geqslant 2\tau_{01} \simeq 800$ sec, giving access to the asymptotic behavior of the transmission rate, if any.

A. Transmitted fraction

We compute the time evolution of the transmitted fraction, $I_{out}(t)/I_{in}$, for various injected current intensities I_{in} ranging from 0.2 to 40 pA. In Figs. 1 and 2, we compare numerical results using $N_{SE} = 2$ to those using $N_{SE} = 0$. For injected currents below 2 pA, the dynamics of the transmitted fraction are sensibility the same in both cases; see Fig. 1. In particular, the asymptotically transmitted fractions, which increase with the injected beam intensity, are quite close. This means that below a certain intensity threshold, which generates only one or two charge patches, the SE channel has no notable influence on the transmission rate and experimental results will not be able to discriminate between both approaches.

For injected intensities above 2 pA, the situation is largely different. First, let us consider the simulated transmission rates using $N_{SE} = 0$, shown in the top panel of Fig. 2. Remarkably, for $I_{in} > 3$, the beam is no longer transmitted continuously from the start. For example, for $I_{in} = 4$, 8, and
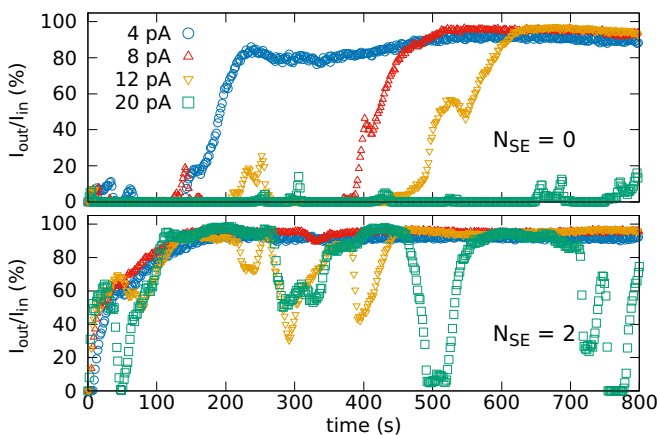

FIG. 2. Simulated transmitted fraction of a 2.5 keV Ar$^+$ ion beam through the 4° tilted capillary as a function of time for different current intensities I_{in} ranging from 4 to 20 pA. Top panel: $N_{SE} = 0$; bottom panel: $N_{SE} = 2$.

12 pA, the beam transmission is mostly blocked during the first 140, 380, and 440 sec, respectively, after which the transmitted fractions increase quickly to the asymptotic value of about 90%. For $I_{in} = 20$ pA, the transmission is outright sparse, with no asymptotic transmission during the first 800 s. For even higher intensities, $I_{in} \geqslant 21$ pA, no transmission is observed. Looking at the trajectories, we found that the beam got stuck in the capillary, while charging the fifth patch (located around $z = 18$ mm) until the beam is Coulomb blocked by the charge patch in the capillary. A movie showing the trapping of the injected beam inside the capillary by charge patches, which attain a potential of U_s, is given in the Supplemental Material [24].

In the bottom panel of Fig. 2, the transmitted fractions were simulated using $N_{SE} = 2$. Unlike the results in the upper panel, for injected intensities $I_{in} = 4$, 8, and 12 pA, the beam is transmitted continuously from start, without interruption. The transmission rates keep following the trend observed in Fig. 1, that is, the beam is transmitted as soon as the first patch is formed, with the asymptotic value increasing with the injected beam intensity. The time evolution of the transmitted fractions for this range of intensities is thus radically different from those without SE. Hence, experimental data should allow us to conclude if a SE source term in the charge dynamics given by Eq. (1) is indeed necessary in order to accurately simulate the patch formation.

Remarkably, for $I_{in} = 20$ pA, the time evolution of the transmitted fraction is no longer continuous, but intermittently blocks for short amounts of time. As can be seen in Fig. 5, the beam gets stuck in the capillary and needs several tens of seconds before the new charge patch is strong enough to deflect the beam out. The Coulomb blocking is, however, avoided for the range of intensities investigated here, $I_{in} \leqslant 40$ pA.

B. Blocking of the transmission

We computed the transmission rates for different values of N_{SE}/q, namely, 1/2, 1, 2, 3, and 4. We increased the current intensity up to 40 pA and checked if the transmission was continuous for at least 800 seconds or if it was blocked for a given period (see, for example, the curve for $I_{in} = 20$ pA in the bottom panel of Fig. 2). The purpose of this study is to investigate the influence of the number of SEs emitted per impact and per ion charge q on the patch formation and resulting guiding. The results are shown in Fig. 3. The blue sticks indicate the range of intensities for which a continuous transmission is monitored once the first patch has been formed, and for which an asymptotic transmitted fraction could be observed; cf. Fig. 1. The orange sticks indicate the range of intensities for which the transmission rate was not continues in time, but blocked intermittently for one or several periods of time. The red sticks give the range of intensities for which Coulomb blocking was observed.

When looking at the height of the blue bars, we note a positive trend with increasing N_{SE}, indicating that a higher current intensity can be transmitted *continuously* if more SE are emitted per ion impact. This trend could be expected from Eq. (5), which tells us that the SE source term scales linearly with N_{SE}. Let us take an injected beam current of $I_{in} = 21$ pA for example: Fig. 3 predicts that such a beam should be
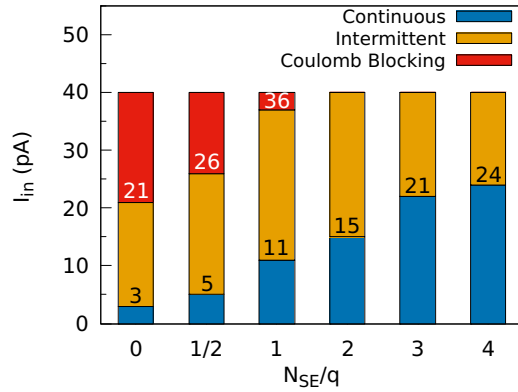
FIG. 3. Blue bars give the range of intensities that yield a continuous transmitted fraction. Orange bars give the range of intensities for which the transmission is intermittently blocked, but asymptotically tends to a stable nonzero transmission. Red bars indicate the range of intensities for which the beam is Coulomb blocked. The ranges of intensities are given for different integer values of N_{SE}.

continuously guided through the tilted capillary if at least, on average, three SE are emitted per impact. On the contrary, with $N_{SE} = 0$, the simulations predict that the beam should be Coulomb blocked inside the capillary. In the case where, on average, 1 or 2 electrons are emitted per ion impact, the beam is expected to be blocked intermittently. The secondary electron channel thus clearly has a non-negligible influence on the time-resolved transmitted fraction, especially in the case of relatively high-intensity ion beams.

C. Ion and electron trajectories

In the following, we will try to explain how the additional SE channel modifies the dynamics of the charge patch formation, resulting in dramatically different time evolution of the transmission rates. The data shown in Fig. 4 are from a simulation using $N_{SE} = 4$, as it visually enhances the statement, but
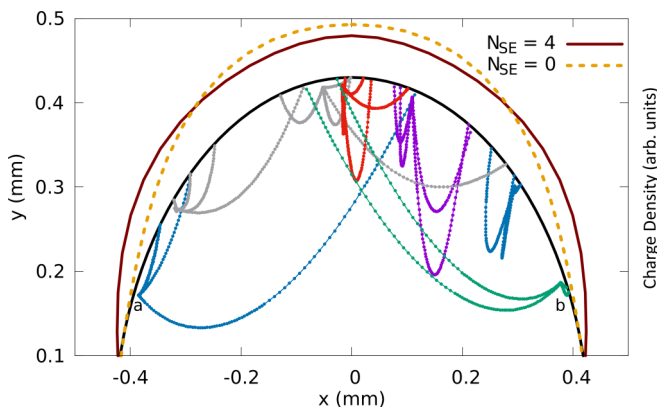

FIG. 4. SE trajectories, projected on the xOy plane for $z \in [0, 10]$ mm (first patch), at the moment $Q_{in} = 40$ pC. The black half circle stands for the inner surface of the radius $R_1 = 0.43$ mm. The brown and the dashed orange curves on top of the black half circle correspond, respectively, to the charge density at the inner surface for $N_{SE} = 4$ SE per ion impact and $N_{SE} = 0$. Labels "a" and "b" indicate two impact points, each emitting four SEs.
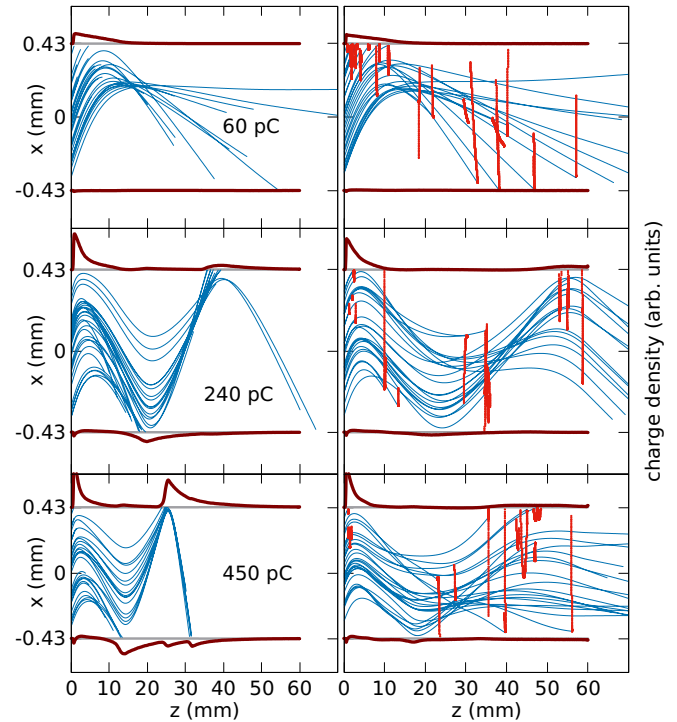

FIG. 5. Snapshots of simulated ion trajectories (blue lines), projected on the xOz plane, taken at different moments and labeled by the injected charge $Q_{in} = 60, 240, 450$ pC. Left panels: without SE, $N_{SE} = 0$. Right panels: two SE per impact were considered, $N_{SE} = 2$. Straight gray lines represent the inner interface of the capillary. The brown curves show the charge density (arb. units) of the charge patches at the inner surfaces. The red lines are the trajectories of SE emitted from the impact points. The injected intensity was $I_{in} = 8$ pA.

the conclusions are also valid for other nonzero values of N_{SE}. We investigate the trajectories of SEs that are emitted from different impact points during the injection of the first charge patch. The latter is located, in our case, typically 3 mm behind the entrance of the capillary; cf. Fig. 5. Let us consider a cut from the cylindrical inner interface by the xOy plane at $z_0 = 3$ mm. In Fig. 4, the cut of the inner surface is represented by the solid black half circle of equation $R_1 \vec{u}_r(\theta)$, where $\vec{u}_r(\theta)$ is the radial unit vector. The brown solid curve on top of the black half circle represents the surface charge distribution $\sigma(\theta, z_0)$, after a charge of $Q_{in} = 40$ pC has been injected. The brown curve is given by the equation $[\sigma(\theta, z_0) + R_1]\vec{u}_r$, so that the difference between the brown and black curves along $\vec{u}_r(\theta)$ gives the surface charge density $\sigma(\theta, z_0)$. The accumulated surface charge distribution generates an electric field (not shown) that drives the emitted electrons.

We show several SE trajectories (colored curves inside the half disk) that have been emitted from different locations of the surface. SEs that are emitted from the central region, labeled "c," "fall" predominantly back to the central region from where they were emitted. Secondary electrons that are emitted from lateral regions label "a" and "b" are predominantly field driven toward the central part "c" of the patch, which is at a higher potential. As a result, the central region "c" accumulates negative charge coming from the lateral regions,

and this flow is proportional to N_{SE}. The SE source term thus tends to redistribute the injected charge more evenly along the angular direction. The difference in the redistribution of the accumulated charge can be appreciated by comparing the cuts of the surface charge distribution with SE (brown solid curve) to the one without SE (orange dashed curve). In terms of moments of the charge injection cross sections [see Eq. (5)], the SE channel tends to decrease the absolute value of the moments γ_{mn} with angular index $m \geqslant 1$, resulting in the formation of a charge patch that is expected to ultimately deflect the ions less that are passing nearby. Note that a redistribution of the injected charge along the axial direction exists too, but is grossly averaged out over the mm-scale long charge patch in the z direction.

We also monitored the trajectories of the injected ions through the capillary. We compare, in Fig. 5, snapshots of the ion trajectories (blue curves) using $N_{\text{SE}} = 2$ (right panels) to those using $N_{\text{SE}} = 0$ (left panels). The red curves shown in the right panels are trajectories of emitted secondary electrons. The gray lines at $x = \pm 0.43$ are cuts of the inner interfaces by the xOz plane. The brown curves on top of the gray lines represent cuts of the surface charge distribution, of equations $\sigma(0, z) + 0.43$ and $-\sigma(\pi, z) - 0.43$. The latter allow us to indicate the location and charge intensity of the charge patches that guide the ions.

After 60 pC have been injected by the 8 pA ion beam, a first charge patch is formed and the ions are deflected towards the opposite wall. While the deflections in the left panel of Fig. 5 (without SE) seem slightly stronger than those in the right panel (with SE), the difference in the transmission rate, up to that moment, is still negligible. After 240 pC have been injected, three patches have already been formed. Now the differences in the trajectories and patch locations between the two approaches are substantial. With SEs, the weaker deflections by the first two patches accumulate, so that the third patch is already located near the exit of the capillary. As a result, a major part of the ions is guided through the capillary. Without SEs, the deflection by the first two patches is notably larger and the third patch is formed about 20 mm from the outlet of the capillary. After 450 pC have been injected, both approaches give completely different results. With SEs, 90% of the injected beam is transmitted, while, without SE (left panel), the beam gets stuck in the middle of the capillary. Except for the first charge patch located near the entrance, which is similar in both approaches, the remaining patches eventually have completely different positions and intensities. Hence, for $N_{\text{SE}} = 2$, the less intense charge patches generate weaker electric fields, which results in smaller beam deflections and thus in further separated charge patches. The lower number of charge patches allow one to guide the beam seamlessly (with less rebounds) through the capillary. The reader will find, in the Supplemental Material, a movie showing the time evolution of the trajectories for the case discussed here [24].

IV. CONCLUSION

We numerically investigated how far SEs alter the dynamics of the patch formation in insulating capillaries, when an ion beam is injected. To this end, we added a SE source term to the surface charge dynamics and simulated the trajectories of the beam ions and SE electrons through a tilted glass tube. We monitored the transmitted fraction of a 2.5 keV Ar$^+$ ion beam through a straight capillary tilted by $4°$ with respect to the beam axis. We varied the beam current over a large range of intensities, from 0.2 to 40 pA, and recorded in time the transmitted fraction. The aim was to make numerical predictions with our code that could be tested experimentally. In order to identify possible trends, the simulations were performed with different numbers of emitted electrons per ion impact, namely, $N_{\text{SE}} = 1/2, 1, \ldots, 4$. We remind the reader that the presented simulations are not only valid for singly charged Ar$^+$ ions, but are also valid for higher charge states q of the Ar ion, if N_{SE} is understood as the number of SE per ion charge state q.

Compared to calculations without SE, we found that the SE channel modifies the distribution of the injected charge, when beam ions hit the insulator surface. In particular, the central part of the patch accumulated SEs coming from lateral impact points, resulting in charge patches that are slightly more uniform, generating weaker electric fields in the vicinity of the patches. Those weaker fields deflect the beam ions less and the charge patches are hence further separated, allowing one to guide the beam through the capillary with less rebounds. We found that a higher SE yield per impact and per ion charge state, N_{SE}/q, has a more pronounced effect on the redistribution of the injected charge, allowing higher beam intensities to be transmitted without experiencing intermittent blocking.

We hope that in the near future, experimental measurements will be able to confirm the crucial role of SE in the self-organized guiding of ion beams by insulating capillaries. On request, we would be delighted to perform calculations for capillaries of different nature and geometry that may be used in dedicated experimental setups.

APPENDIX: DIMENSIONLESS EQUATIONS

1. Equation of motion

We consider an ion of charge q and mass m, extracted by a potential U_s. The initial velocity of the ion is $v_0 = \sqrt{2qU_s/m}$. Only the electric field generated by the deposited charge in the capillary wall acts on the ion. Other forces such as the image charge force at the vacuum-glass interface are ignored. Introducing the characteristic time t_0, the equation of motion (EOM) of an ion can be put into a dimensionless form,

$$\frac{d\vec{\tilde{v}}}{d\tilde{t}} = \frac{t_0}{v_0} \frac{q}{m} \frac{U_s}{H} \vec{\tilde{E}} \quad \text{with} \begin{vmatrix} \vec{\tilde{v}} &= \vec{v}/v_0 \\ \tilde{t} &= t/t_0 \\ \vec{\tilde{E}} &= \vec{E}(H/U_s), \end{vmatrix} \tag{A1}$$

where the tilted quantities are dimensionless. Defining the characteristic time $t_0 = \frac{1}{2} v_0 \, mH/(qU_s) = H/v_0$, the equation

of motion (EOM)

$$\frac{d\vec{\tilde{v}}}{d\tilde{t}} = \frac{1}{2}\vec{\tilde{E}} \qquad (A2)$$

becomes independent of q or m of the ion as well as of the extraction potential of the source U_s. The trajectory of the ions depends only on its initial trace-space conditions, that is, on the initial position $\vec{r}$ and initial direction of the velocity vector $\vec{v}_0/v_0$.

2. Surface charge dynamics

In this section, we want to identify the parameters that control the dynamics of the surface charge density given by Eq. (3) and show that the dynamics depend explicitly on the ratios U_s/I_{in} and N_{SE}/q. Let us first define the characteristic surface charge density σ_0,

$$\sigma_0 = \frac{C U_s}{S_1} = \frac{\varepsilon_0 \varepsilon_r U_s}{R_1 \ln \frac{R_2}{R1}}, \qquad (A3)$$

where $C = 2\pi\varepsilon_0\varepsilon_r H/\ln\frac{R_2}{R1}$ and $S_1 = 2\pi R_1 H$ are, respectively, the capacity and inner surface of the capillary. Introducing the characteristic charging time τ_c as well as the characteristic current density I_{in}/S_1, Eq. (3) may be written in the following form:

$$\frac{\sigma_0}{\tau_c}\frac{\partial\tilde{\sigma}_{mn}}{\partial\tilde{t}} = -\frac{\sigma_0}{\tau_{mn}}\tilde{\sigma}_{mn} + \frac{I_{\text{in}}}{S_1}\tilde{\gamma}_{mn}, \qquad (A4)$$

where the tilded quantities are dimensionless. Defining

$$\begin{aligned}
\tau_c &= \frac{S_1}{I_{\text{in}}}\sigma_0 \\
&= \underbrace{\left(\frac{U_s}{I_{\text{in}}}\right)}_{\text{beam}}\underbrace{\left(\frac{\varepsilon_0\varepsilon_r\pi H}{\ln\frac{R_2}{R1}}\right)}_{\text{capillary}}
\end{aligned} \qquad (A5)$$

allows us to write Eq. (A4) in dimensionless form,

$$\frac{\partial\tilde{\sigma}_{mn}}{\partial\tilde{t}} = -\frac{\tau_c}{\tau_{mn}}\tilde{\sigma}_{mn} + \tilde{\gamma}_{mn}. \qquad (A6)$$

From the definition of τ_c, we see that the charge dynamics depend on the ratio U_s/I_{in}. Consequently, although the EOM does not depend on the beam parameters U_s and I_{in}, the transmission rate eventually depends on their ratio via Eq. (A6). Injecting the source term given by Eq. (5) into Eq. (A6), one finally gets

$$\frac{\partial\tilde{\sigma}_{mn}}{\partial\tilde{t}} = -\frac{\tau_c}{\tau_{mn}}\tilde{\sigma}_{mn} + \left\{\tilde{\gamma}_{mn}^h + \frac{N_{\text{SE}}}{q}\left[\tilde{\gamma}_{mn}^h(t) - \tilde{\gamma}_{mn}^e(t)\right]\right\}. \qquad (A7)$$

Because of the added SE source term, the charge dynamics and thus the transmission now also depend on the ratio N_{SE}/q.

[1] N. Stolterfoht, J.-H. Bremer, V. Hoffmann, R. Hellhammer, D. Fink, A. Petrov, and B. Sulik, Transmission of 3 keV Ne^{7+} Ions through Nanocapillaries Etched in Polymer Foils: Evidence for Capillary Guiding, Phys. Rev. Lett. **88**, 133201 (2002).

[2] T. Ikeda, Y. Kanai, T. M. Kojima, Y. Iwai, T. Kambara, and Y. Yamazaki, M. Hoshino, T. Nebiki, and T. Narusawa, Production of a microbeam of slow highly charged ions with a tapered glass capillary, Appl. Phys. Lett. **89**, 163502 (2006).

[3] K. Schiessl, W. Palfinger, K. Tőkési, H. Nowotny, C. Lemell, and J. Burgdörfer, Simulation of guiding of multiply charged projectiles through insulating capillaries, Phys. Rev. A **72**, 062902 (2005).

[4] N. Stolterfoht, Simulation and analysis of ion guiding through a nanocapillary in insulating polymers, Phys. Rev. A **87**, 012902 (2013).

[5] N. Stolterfoht, Simulations and analytic models of ion guiding through a nanocapillary in insulating polymers, Phys. Rev. A **87**, 032901 (2013).

[6] N. Stolterfoht, Simulations of ion-guiding through insulating nanocapillaries of varying diameter: Interpretation of experimental results, Atoms **8**, 48 (2020).

[7] N. Stolterfoht, Simulations of ion guiding through a straight macrocapillary: Interpretation of an experiment and comparison with nanocapillaries, Phys. Rev. A **89**, 062706 (2014).

[8] N. Stolterfoht, E. Gruber, P. Allinger, S. Wampl, Y. Wang, M. J. Simon, and F. Aumayr, Experiments and simulations of 4.5-keV Ar^{7+}–ion guiding through a conical glass microcapillary, Phys. Rev. A **91**, 032705 (2015).

[9] E. Giglio, S. Guillous, and A. Cassimi, Ion-beam focusing by self-organized axis-symmetric potentials in insulating capillaries, Phys. Rev. A **98**, 052704 (2018).

[10] E. Giglio and M. Léger, Stabilizing the ion beam transmission through tapered glass capillaries, arXiv:2103.07730v1.

[11] R. D. DuBois, K. Tőkési, and E. Giglio, Charge deposition, redistribution, and decay properties of insulating surfaces obtained from guiding of low-energy ions through capillaries, Phys. Rev. A **99**, 062704 (2019).

[12] K. Schiessl, K. Tőkési, B. Solleder, C. Lemell, and J. Burgdörfer, Electron Guiding through Insulating Nanocapillaries, Phys. Rev. Lett. **102**, 163201 (2009).

[13] http://www.warneronline/product/236.

[14] E. Giglio, Charge relaxation rates in insulating straight capillaries, Phys. Rev. A **101**, 052707 (2020).

[15] E. Giglio, K. Tőkési, and R. D. DuBois, Relaxation dynamics of charge patches formed inside an insulating capillary by ion impact, Nucl. Instrum. Methods B **460**, 234 (2019).

[16] E. Gruber, G. Kowarik, F. Ladinig, J. P. Waclawek, D. Schrempf, F. Aumayr, R. J. Bereczky, K. Tőkési, P. Gunacker, T. Schweigler, C. Lemell, and J. Burgdörfer, Temperature control of ion guiding through insulating capillaries, Phys. Rev. A **86**, 062901 (2012).

[17] K. Floettmann, Some basic features of the beam emittance, Phys. Rev. ST Accel. Beams **6**, 034202 (2003).

[18] W. Meissl et al., Electron emission from insulators irradiated by slow highly charged ions, e-J. Surf. Sci. Nanotech. **6**, 54 (2008).

[19] J. Mischler, N. Benazeth, M. Nègre, and C. Benazeth, Angular distributions of secondary electrons emitted in Ar+-Polycrystalline al collisions, Surf. Sci. **136**, 532 (1984).

[20] J. Greenwood, The correct and incorrect generation of a cosine distribution of scattered particles for Monte-Carlo modelling of vacuum systems, Vacuum **67**, 217 (2002).

[21] M. A. Furman and M. T. F. Pivi, Probabilistic model for the simulation of secondary electron emission, Phys. Rev. ST Accel. Beams **5**, 124404 (2002); **16**, 069901 (2013).

[22] N. Colombie, C. Benazeth, J. Mischler, and L. Viel, Angular and energetic distributions of secondary electrons emitted by solid targets under ionic bombardment, Radiat. Effects **18**, 251 (1973).

[23] E. Schreiber and H.-J. Fitting, Monte Carlo simulation of secondary electron emission from the insulator SiO$_2$, J. Electron Spectrosc. Relat. Phenom. **124**, 25 (2002).

[24] See Supplemental Material at http://link.aps.org/supplemental/10.1103/PhysRevA.103.032825 for a movie (`ion_traj_blocking_I24.gif`) showing how the trajectories (in blue) evolve with the evolving surface charge density (in brown). The top panel uses $N_{SE} = 0$. The injected beam is blocked inside the capillary. The bottom panel uses $N_{SE} = 2$. The injected beam is continuously transmitted. The injected intensity is 24 pA. Also, see the other movie (`ion_traj_I12.gif`) showing how the trajectories (in blue) evolve with the evolving surface charge density (in brown). The top panel uses $N_{SE} = 0$. Multiple patches are generated, but, this time, the injected beam gets eventually transmitted. The bottom panel uses $N_{SE} = 2$. The injected beam is continuously transmitted. The injected intensity is 12 pA.